WAKEFIELD COMPUTATIONS FOR THE CLIC PETS USING THE PARALLEL FINITE ELEMENT TIME-DOMAIN CODE T3P *

A. Candel†, A. Kabel, L. Lee, Z. Li, C. Ng, G. Schussman and K. Ko,
SLAC, Menlo Park, CA 94025, U. S. A.

I. Syratchev, CERN, Geneva, Switzerland

Abstract

In recent years, SLAC's Advanced Computations Department (ACD) has developed the high-performance parallel 3D electromagnetic time-domain code, T3P, for simulations of wakefields and transients in complex accelerator structures. T3P is based on advanced higher-order Finite Element methods on unstructured grids with quadratic surface approximation. Optimized for large-scale parallel processing on leadership supercomputing facilities, T3P allows simulations of realistic 3D structures with unprecedented accuracy, aiding the design of the next generation of accelerator facilities. Applications to the Compact Linear Collider (CLIC) Power Extraction and Transfer Structure (PETS) are presented.

CLIC PETS STRUCTURE

In the following, time-domain wakefield simulations of the X-Band (12 GHz) CLIC PETS are presented. The PETS is one of the two key components of the proposed CLIC two beam scheme for high RF transfer efficiency: A low energy, high current drive beam passes through the passive PETS and supplies RF power to the main beam.

The PETS is a periodically loaded traveling wave structure with an active length of 21.3 cm (34 cells), a period of 6.253 mm (90°/cell) and an aperture of 23 mm [1]. It is assembled from 8 identical sectors separated by radial slots with embedded lossy dielectric loads required to dampen the transverse wakefields that would otherwise destroy the drive beam quality.

The current CLIC design requires over 35,000 PETS per Linac and careful design and optimization is critical to the overall success of the project. Numerical simulations are required to quantitatively investigate the wakefield impedance from loading of the dielectric absorbers.

SIMULATION CODE T3P

In the following, a brief introduction to the employed methods for modeling the electromagnetic fields generated by a particle beam in an accelerator structure is given. The simulation code T3P solves the full set of Maxwell's equations in time domain and includes retardation and boundary effects first principles.

Maxwell Finite Element Time-Domain

In our approach, Ampère's and Faraday's laws are combined and integrated over time to yield the inhomogeneous vector wave equation for the time integral of the electric field $\mathbf{E}$:

$$\left(\varepsilon\frac{\partial^2}{\partial t^2}+\sigma_{\rm eff}\frac{\partial}{\partial t}+\nabla\times\mu^{-1}\nabla\times\right)\int^{\mathbf{t}}\mathbf{E}\,\mathrm{d}\tau=-\mathbf{J},\quad(1)$$

with permittivity ε=$\varepsilon_0\varepsilon_r$ and permeability μ=$\mu_0\mu_r$. For simplicity in the computations, a constant value of the effective conductivity $\sigma_{\rm eff}$=$\tan\delta\cdot 2\pi \mathrm{f}\cdot\varepsilon$ is assumed by fixing a frequency f, and the losses are specified by the loss tangent $\tan\delta$. As is common for wakefield computations of rigid beams, the electric current source density $\mathbf{J}$ is given by a one-dimensional Gaussian particle distribution, moving at the speed of light along the beam line.

The computational domain is discretized into curved tetrahedral elements and $\int^t\mathbf{E}\,\mathrm{d}\tau$ in Eq. (1) is expanded into a set of hierarchical Whitney vector basis functions $\mathbf{N_i}(\mathbf{x})$ up to order p within each element:

$$\int^t\mathbf{E}(\mathbf{x},\tau)\,\mathrm{d}\tau=\sum_{i=1}^{N_p}e_i(t)\cdot\mathbf{N_i}(\mathbf{x}).\quad(2)$$

For illustration, N_2=20 and N_6=216. Higher-order elements not only significantly improve field accuracy and dispersive properties [2], but they also generically lead to higher-order accurate particle-field coupling equivalent to, but much less laborious than, complicated higher-order interpolation schemes commonly found in finite-difference methods.

After accounting for boundary conditions at domain boundaries, e.g. metallic cavity walls or symmetry planes, and consistency between neighboring elements, a global number of expansion coefficients is obtained, representing the field degrees of freedom (DOFs) of the system.

Substituting Eq. (2) into Eq. (1), multiplying by a test function and integrating over the computational domain Ω results in a system of linear equations, second-order in time. Partial integration leads to additional boundary terms. The implicit Newmark-Beta scheme [3] is employed for numerical time integration. It is unconditionally stable,

* Work supported by the U. S. DOE ASCR, BES, and HEP Divisions under contract No. DE-AC002-76SF00515.

† candel@slac.stanford.edu

i.e. the largest allowable time step does not depend on the smallest mesh size in the overall computational domain. The resulting (parallelly distributed) matrix is factorized either directly or iteratively using the conjugate gradient approach with a suitable preconditioner. Currently, iterative methods exhibit better parallel scalability and are the preferred method for solving large problems.

At a given discrete time t, the electric field $\mathbf{E}$ and the magnetic flux density $\mathbf{B}$ are easily obtained from the solution vector $\mathbf{e}$:

$$\mathbf{E}(\mathbf{x}) = \sum_{\mathbf{i}} (\partial_{\mathbf{t}} \mathbf{e})_{\mathbf{i}} \cdot \mathbf{N_i}(\mathbf{x}) \tag{3}$$

and

$$\mathbf{B}(\mathbf{x}) = -\sum_{\mathbf{i}} (\mathbf{e})_{\mathbf{i}} \cdot (\nabla \times \mathbf{N_i}(\mathbf{x})) \,. \tag{4}$$

More detailed information about the methods used in T3P has been published earlier [4].

T3P VALIDATION

For validation purposes, wakefields are calculated for a simple synthetic test case with lossy dielectric material. T3P results are compared with results from the well established time-domain code MAFIA T2. The geometry is a cylindrical pillbox (length and radius are both 6 cm) with a beam pipe of 2 cm radius. An annulus with lossy dielectric material properties (ε_r=15, μ_r=1, σ_{eff}=2/3) is placed in the cavity. A Gaussian bunch of σ_z=1cm is driven along center of the beam pipe in z-direction, and the resulting longitudinal wake potential is calculated using Weiland's method [5]. Since the problem is cylindrically symmetric, accurate results are easily obtained with the 2D code MAFIA T2.

Figure 1 shows the mesh model used for T3P calculations in 3D, a 10 degree slice, and magnetic boundary conditions are applied to enforce cylindrical symmetry. In both codes, the computational mesh size and time step are chosen to be small enough to reach convergence, and the mesh in the absorber region is refined accordingly in order to be able to resolve the smaller wavelengths. The beam pipe is truncated at both ends with absorbing boundary conditions. In order to reduce numerical boundary condition errors, truncation is done far enough away from the cavity, i.e. at several times the beam pipe radius.

Figure 2 shows the excellent agreement between T3P and MAFIA T2 results.

T3P PETS MESH MODEL

All mesh-based electromagnetic time-domain simulations depend on adequate discretization of the calculation domain, particularly of the material boundaries, especially when scattering phenomena are modeled. Simulation accuracy generally improves with finer meshes and better boundary approximations.

T3P is based on unstructured meshes of up to second-order curved tetrahedral elements – this allows modeling

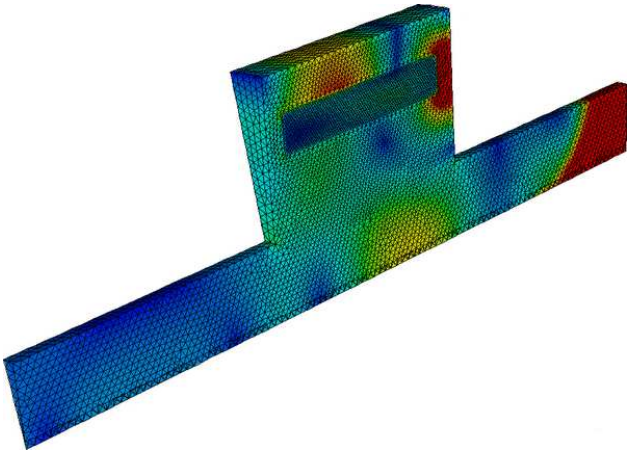

Figure 1: Unstructured conformal tetrahedral mesh model of a 10 degree slice of the validation test case, as used for calculations with T3P. The mesh is refined in the region of the lossy material. The beam is about to leave the geometry and the excited wakefields are visible.

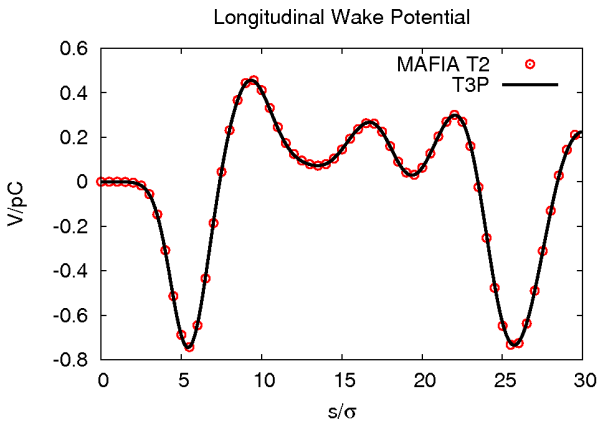

Figure 2: Longitudinal wake potential for the lossy pillbox validation case (ϵ=15, μ=1, σ=2/3). There is excellent agreement between T3P and MAFIA T2 results, as expected from the cylindrically symmetric test case and the convergence behavior of the codes.

of small geometric features and scattering effects with high accuracy. In combination with higher-order field representation, highly efficient use of computational resources and unprecedented simulation accuracy are obtained.

Figures 3 and 4 show detailed views of a high-quality mesh model of the full PETS with 34 regular cells, 2 matching cells, outer tank, and output coupler. A model of one symmetric quadrant of the PETS requires roughly 9 million tetrahedral elements, with an average mesh resolution of about 1 mm and down to 0.3 mm for the dielectric loads (ε_r=24, μ_r=1), which require a locally refined mesh for proper resolution of the smaller resulting wavelengths. This mesh is used for most of the calculations performed with T3P that are presented in the following.

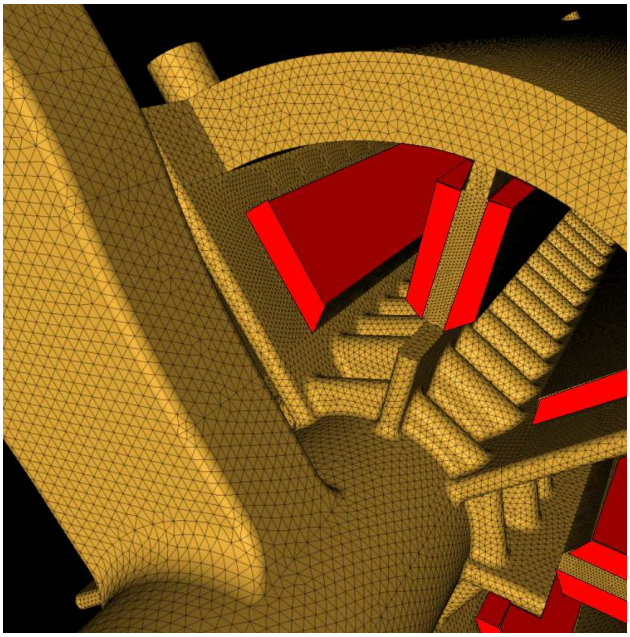

Figure 3: External view of the unstructured conformal tetrahedral mesh model of the PETS, used for T3P calculations. Visible are the beam pipe with several regular cells and the matching cell, the output coupler as well as the outer tank. The dielectric loads are highlighted in red. The corresponding mesh region is locally refined for improved resolution of the smaller resulting wavelengths.

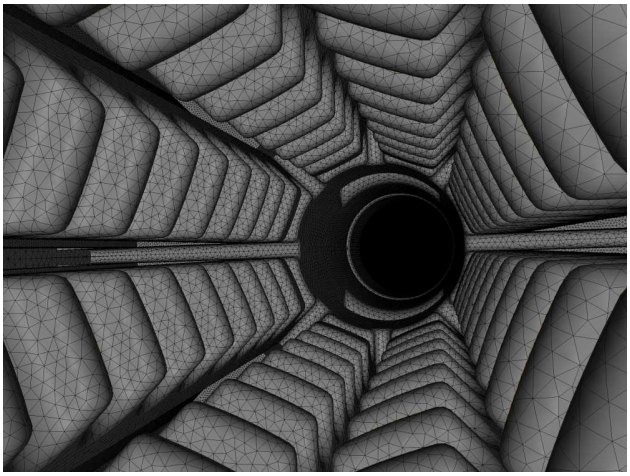

Figure 4: Unstructured conformal tetrahedral mesh model of the PETS, used for T3P calculations. From this viewpoint close to the beam line axis, the curved cell irises, the slots and the output coupler openings are visible.

T3P PETS WAKEFIELD CALCULATIONS

Using the aforementioned PETS model, wakefield calculations have been performed with T3P. Since the main interest is on transverse wakefields, a Gaussian current is driven along the beam pipe axis (the z-direction) with an x-offset of 2.5 mm and beam parameters σ_z=2 mm, $\pm 3\sigma_z$. This is equivalent to a pure dipole current by enforcing electric boundary conditions on the yz-symmetry plane. For simplicity, the same basis order p is used for all mesh elements and the effective conductivity is calculated with f=12 GHz.

Figure 5 shows one half of the structure with a snapshot of the excited wakefields on the surfaces. The transverse wake potential is obtained from the longitudinal wake potential by applying the Panofsky-Wenzel theorem [6], which requires an integration of the longitudinal wake potential.

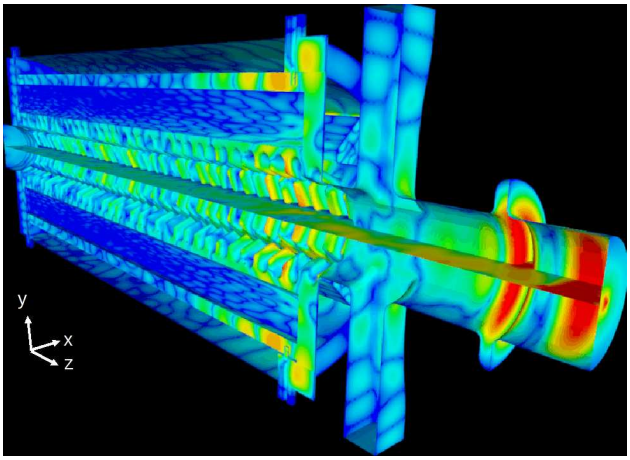

Figure 5: Snapshot of excited wakefields calculated by T3P as the beam is about to leave the PETS. Electric cut plane at x=0 excludes monopole modes. The magnetic symmetry plane y=0 is shown for visualization purposes, it includes the beam with an offset of x=2.5 mm. Strong damping in the lossy dielectric loads (ε_r=24, $\tan\delta$=0.32) is directly observed, as well as some fields in the output coupler and choke.

Figure 6 shows the convergence of the transverse wake potential as a function of the order p of the Finite Element basis functions.

Figure 7 shows the convergence behavior in frequency domain, where the absolute value of the transverse impedance (Fourier transform of the wake potential of a point charge) is plotted instead. Results from p=1 calculations are the least accurate and show differences to calculations with p=2 and p=3, which are almost identical. Results for p=1 are obtained within a few hundred CPU hours, while p=3 requires several tens of thousands of CPU hours on massively parallel supercomputers (thousands of CPUs). Results with p=2 require in the order of a few thousand CPU hours and can be considered well converged for purposes of this study. Consequently, all computations with T3P are performed with Finite Element basis order p=2 in the following.

Convergence in the field integration time step has been observed as well, and a time step of 0.5 ps was required to reach convergence for p=2. This corresponds to a spatial resolution of hundreds of microns and allows modeling of the smallest features in the geometry with high accuracy.

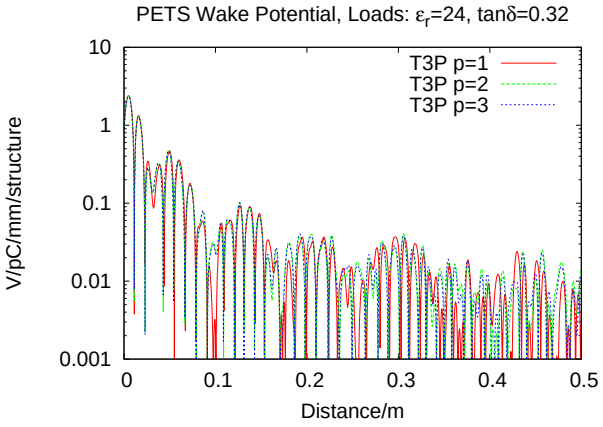

Figure 6: Convergence of transverse wake potential as a function of the order p of the Finite Element basis functions used in T3P calculations.

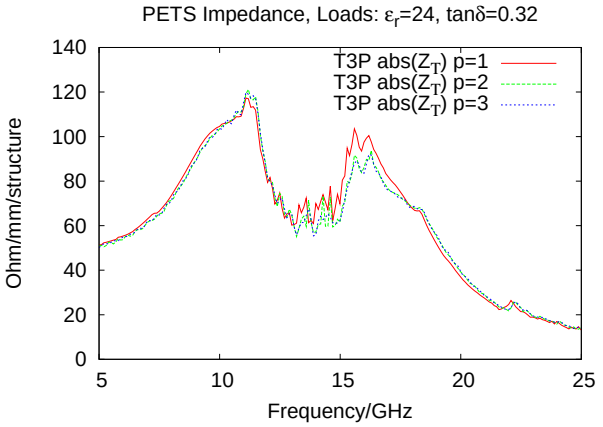

Figure 7: Convergence of transverse impedance as a function of the order p of the Finite Element basis functions used in T3P calculations.

Figure 8 shows the effect of the lossy dielectric loads by comparing the transverse wake potential with and without losses ($\tan\delta$=0.32 vs $\tan\delta$=0, c.f. Eq. (1)). The dielectric properties and permeability of the absorber material are kept constant, i.e. ε_r=24, μ_r=1). A drop of about one order of magnitude in the wakefield amplitudes is observed after about one active length if losses are enabled.

COMPARISON OF T3P AND GDFIDL

Finally, T3P results are compared to GdfidL results [1]. GdfidL is a parallel electromagnetic time-domain code based on the conventional finite difference scheme on structured rectilinear grids. Similar to MAFIA, GdfidL features first-order boundary approximation (cut-cells) and first-order field representation.

For simplicity, the output coupler and the outer tank are omitted for the comparison simulations. All other parameters remain the same, including beam and material properties. T3P calculations are performed with Finite Element basis order p=2.

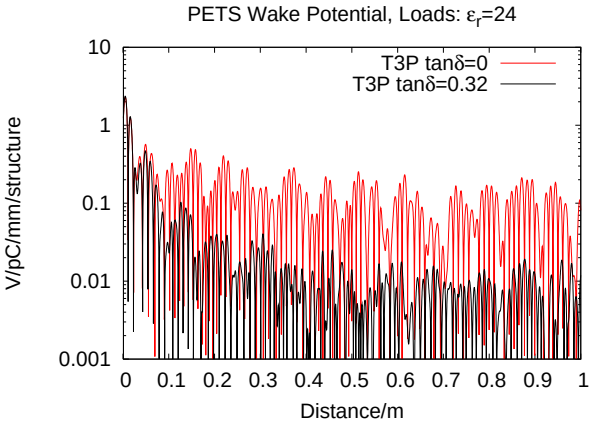

Figure 8: Impact of absorbers on the transverse wake potential. The lossless case ($\tan\delta$=0) is compared to the lossy case with $\tan\delta$=0.32.

Figure 9 shows the geometry of the simplified PETS model.

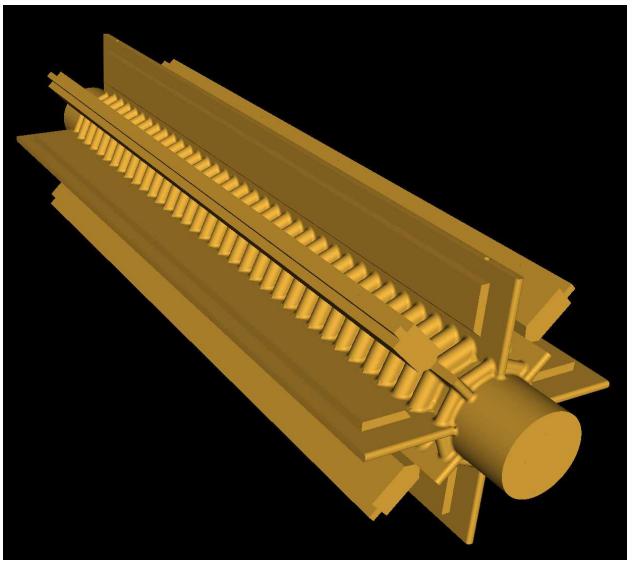

Figure 9: Simplified PETS model without outer tank and output coupler, for comparison simulations between T3P and GdfidL.

Figures 10 and 11 show the transverse wake potentials and impedances as calculated with T3P and GdfidL. Good general agreement between the codes is found. GdfidL results show relative deviations from the T3P results (with p=2), in magnitude and features comparable to the ones between p=1 and p=2 in earlier T3P runs, while with slightly different geometry (no coupler, no outer tank). This finding is consistent with GdfidL's general first-order approach – further corroborating the applicability of our methods.

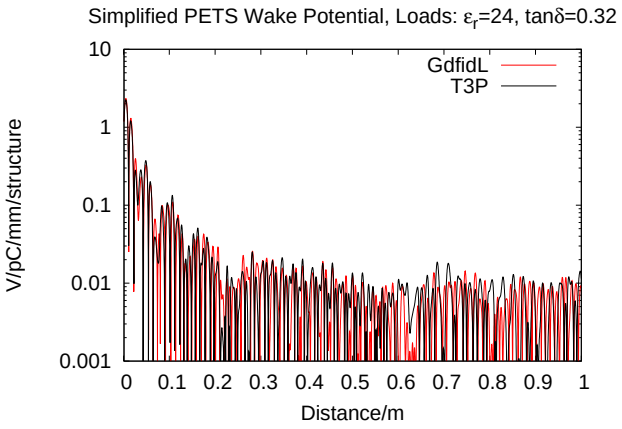

Figure 10: Comparison of transverse wake potential calculated with GdfidL and T3P for the simplified PETS geometry from Fig. 9.

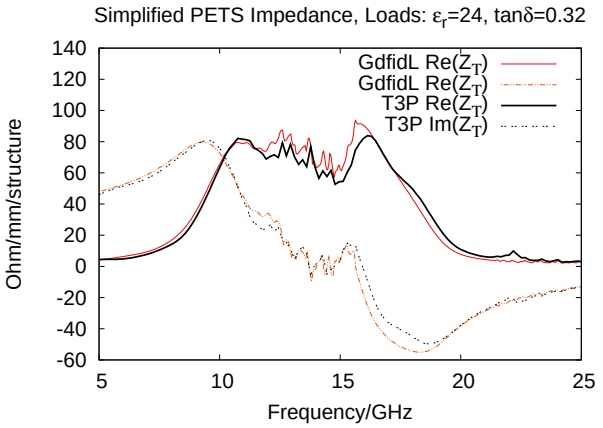

Figure 11: Comparison of transverse impedance calculated with GdfidL and T3P for the simplified PETS geometry from Fig. 9.

SUMMARY

SLAC's parallel Finite Element 3D electromagnetic time-domain code T3P employs state-of-the-art parallel Finite Element methods on curved conformal unstructured meshes with higher-order field representation. T3P allows large-scale time-domain simulations of complex, realistic 3D structures with unprecedented accuracy, aiding the design and operation of the next generation of accelerator facilities. T3P has been extensively benchmarked against established codes. In this study, T3P has been used to calculate transverse wakefield damping effects in the CLIC PETS, which involves lossy materials and complex geometric features. Thanks to access to large-scale computational resources, and due to the unique features of T3P, convergence of the results could be achieved.

ACKNOWLEDGMENTS

This work was supported by the US DOE ASCR, BES, and HEP Divisions under contract No. DE-AC002-76SF00515. This research used resources of the National Energy Research Scientific Computing Center, and of the National Center for Computational Sciences at Oak Ridge National Laboratory, which are supported by the Office of Science of the U. S. Department of Energy under Contract No. DE-AC02-05CH11231 and No. DE-AC05-00OR22725. – We also acknowledge the contributions from our SciDAC collaborators in numerous areas of computational science.

REFERENCES

[1] I. Syratchev, "PETS and drive beam development for CLIC", Proc. X-Band RF Structure and Beam Dynamics Workshop, Daresbury, UK, Dec 1-4, 2008.

[2] M. Ainsworth, "Dispersive properties of high-order Nedelec/edge element approximation of the time-harmonic Maxwell equations", Philos. trans.-Royal Soc., Math. phys. eng. sci., vol. 362, no. 1816, pp. 471-492, 2004.

[3] N. M. Newmark, "A method of computation for structural dynamics", Journal of Eng. Mech. Div., ASCE, vol. 85, pp. 67-94, July 1959.

[4] A. Candel et al., "Parallel Higher-order Finite Element Method for Accurate Field Computations in Wakefield and PIC Simulations", Proc. ICAP 2006, Chamonix Mont-Blanc, France, October 2-6, 2006.

[5] T. Weiland, "Transient Electromagnetic Fields Excited by Bunches of Charged Particles in Cavities of Arbitrary Shape", Proc. International Conference on High Energy Accelerators (CERN 1980), July 7, 1980, pp. 570-575.

[6] W. K. H. Panofsky and W. A. Wenzel, "Some Considerations Concerning the Transverse Deflection of Charged Particles in Radio-Frequency Fields", Review of Scientific Instruments, vol. 27, pp. 967-+, November 1956.